



ELSEVIER

17 May 2001

Physics Letters B 507 (2001) 115–120

PHYSICS LETTERS B

www.elsevier.nl/locate/npe

# Transition quadrupole moments in $\gamma$ -soft nuclei and the triaxial projected shell model

Javid A. Sheikh<sup>a</sup>, Yang Sun<sup>b,c,d</sup>, Rudrajyoti Palit<sup>e</sup>

<sup>a</sup> Physik-Department, Technische Universität München, D-85747 Garching, Germany

<sup>b</sup> Department of Physics and Astronomy, University of Tennessee Knoxville, Tennessee 37996, USA

<sup>c</sup> Department of Physics, Tsinghua University, Beijing 100084, PR China

<sup>d</sup> Department of Physics, Xuzhou Normal University Xuzhou, Jiangsu 221009, PR China

<sup>e</sup> Tata Institute of Fundamental Research, Colaba, Bombay 400005, India

Received 1 March 2001; accepted 5 March 2001

Editor: W. Haxton

## Abstract

Transition probabilities of the ground-state bands in  $\gamma$ -soft nuclei are studied for the first time using the triaxial projected shell model approach. It is observed that the angular-momentum dependence of the transition quadrupole moment  $Q_t$  is related to the triaxial deformation of the nuclear mean-field potential. The introduction of the  $\gamma$ -degree of freedom in the shell model basis is shown to have a little influence on the *constant* behavior of the low-spin  $Q_t$  in a well-deformed nucleus. However, the *increasing* collectivity with spin for the low-spin states in a  $\gamma$ -soft nucleus can only be explained by considering the triaxial mean-field deformation. © 2001 Elsevier Science B.V. All rights reserved.

The study of the nuclear shape as a function of angular momentum has remained in the forefront of the nuclear physics research. The study of transition probabilities plays an important role in our understanding of the shape evolution. For instance, probability of the electric quadrupole transition directly reflects the deformation of a nuclear system. For a spherical nucleus, the electric quadrupole transition is of the order of a Weisskopf unit, whereas for a deformed system the transition is several hundred times the Weisskopf estimate [1]. Nuclear deformation is also believed to be one of the most important physical quantities in the astrophysical interest [2]. Many nuclei in nuclear periodic table exhibit axially symmetric deformation in their ground state, with the projection of angular mo-

mentum on the symmetry axis as a conserved quantum number. This is referred to as the  $K$  quantum number and the rotational bands are labelled with this quantum number. In fact, the majority of electromagnetic transitions in nuclei are found to strictly obey the selection rules based on the  $K$  quantum number [1]. The violation of  $K$ -selection rules is an indication that the system is not axially symmetric. This has been demonstrated, for example, in high- $K$  isomeric states [3].

Well-deformed nuclei, in particular those in the heavy mass regions, exhibit the characteristics of an axially symmetric-rotor in the low-spin states of their ground-band (g-band). For example, in well-deformed rare-earth nuclei, the transition quadrupole moments  $Q_t$  usually show a constant behavior for the spin range  $0 \leq I \leq 10$ , before the first band crossing. This behavior has been found in many calculations

E-mail address: yang@csep10.phys.utk.edu (Y. Sun).

with the cranked mean-field models (see, for example, Ref. [4]) and also in those with angular momentum projection [5–7].

However, the properties of quadrupole moments for nuclei in the transitional regions have been less understood. There has been a long-standing problem in nuclear structure physics: what are the fingerprints of triaxial deformation in the electromagnetic transition probabilities in the g-bands for transitional nuclei? In the present work, we would like to address this question. It is demonstrated that the angular momentum dependence of the transition quadrupole moments for the low-spin states can provide a measure of the triaxial deformation.

The nuclei discussed here with neutron number around 90 have g-bands that are quasi-rotational with considerable vibrational character. The ground-state energy surface of these transitional nuclei has been shown to have a shallow minimum at a finite  $\gamma$ -deformation in the Hartree–Fock–Bogoliubov (HFB) calculations [8]. It was demonstrated that such a shallow minimum becomes a prominent one when projected onto spin  $I = 0$  [9]. Thus, to describe these transitional nuclei, it is important to consider the basis-states which are eigenstates of the triaxial mean-field potential rather than axial basis used in most of the earlier studies [10]. The necessity of introducing triaxiality to describe the observed g-band moment of inertia of transitional nuclei has recently been demonstrated [11]. The restriction to an axially deformed basis in the projected shell model approach [10] was released by performing three-dimensional angular momentum projection on the triaxial deformed basis. This approach has been referred to as the triaxial projected shell model (TPSM). It was shown that the observed steep increase of moment of inertia for transitional nuclei can be well described [11] by considering  $\gamma$ -deformation. It was found later [12] that, with the same triaxial deformation, the first excited TPSM band describes also the observed  $\gamma$ -vibrational band, and the second excited TPSM band reproduces the experimental  $\gamma\gamma$ -band.

In the present work, the transition quadrupole moments  $Q_t$  are studied for the first time by using the TPSM. In this approach, the states with good angular momentum are obtained by projection from the triaxial Nilsson wave-function using the three-dimensional angular momentum projection method. Here, our in-

terest lies in the low-spin states with  $0 \leq I \leq 10$  before the quasi-particle (qp) alignments, and therefore, we shall restrict our many-body basis to the angular momentum projected triaxial qp-vacuum state:

$$\{\hat{P}_{MK}^I|\Phi\rangle, 0 \leq K \leq I\}, \quad (1)$$

where  $\hat{P}_{MK}^I$  is the projection operator

$$\hat{P}_{MK}^I = \frac{2I+1}{8\pi^2} \int d\Omega D_{MK}^I(\Omega) \hat{R}(\Omega), \quad (2)$$

and  $|\Phi\rangle$  represents the triaxial qp vacuum state. This is the simplest possible configuration space for an even-even nucleus. It should be noted that for the case of axial symmetry, the qp-vacuum state has  $K = 0$ , whereas in the present case with triaxial deformation, the vacuum state has all possible  $K$  values. The rotational bands based on the triaxial vacuum state are obtained by specifying different values for the  $K$  quantum number in the rotational  $D$ -matrix. The allowed values of the  $K$  quantum number for a given intrinsic state are determined through the following symmetry requirement. For  $\hat{S} = e^{-i\pi\hat{J}_z}$ , we have

$$\hat{P}_{MK}^I|\Phi\rangle = \hat{P}_{MK}^I \hat{S}^\dagger \hat{S}|\Phi\rangle = e^{i\pi(K-\kappa)} \hat{P}_{MK}^I|\Phi\rangle, \quad (3)$$

where  $\hat{S}|\Phi\rangle = e^{-i\pi\kappa}|\Phi\rangle$ . For the self-conjugate vacuum state,  $\kappa = 0$  and, therefore, it follows from Eq. (3) that only even-values of  $K$  are permitted.

As in the earlier PSM calculations, we use the pairing plus quadrupole–quadrupole Hamiltonian [10]

$$\begin{aligned} \hat{H} = \hat{H}_0 - \frac{1}{2}\chi \sum_{\mu} \hat{Q}_{\mu}^{\dagger} \hat{Q}_{\mu} - G_M \hat{P}^{\dagger} \hat{P} \\ - G_Q \sum_{\mu} \hat{P}_{\mu}^{\dagger} \hat{P}_{\mu}. \end{aligned} \quad (4)$$

The corresponding triaxial Nilsson Hamiltonian is given by

$$\hat{H}_N = \hat{H}_0 - \frac{2}{3}\hbar\omega \left\{ \epsilon \hat{Q}_0 + \epsilon' \frac{\hat{Q}_{+2} + \hat{Q}_{-2}}{\sqrt{2}} \right\}. \quad (5)$$

In Eq. (4),  $\hat{H}_0$  is the spherical single-particle Hamiltonian, which contains a proper spin–orbit force [13]. For the axial deformation  $\epsilon$  in the Nilsson model, we take the values given in Ref. [14]. The interaction strengths are taken as follows: the  $QQ$ -force strength  $\chi$  is adjusted such that the quadrupole deformation  $\epsilon$  is obtained as a result of the self-consistent mean-field

HFB calculation [10]. The monopole pairing strength  $G_M$  is of the standard form  $G_M = [21.24 \mp 13.86 \times (N - Z)/A]/A$ , with “−” for neutrons and “+” for protons, which approximately reproduces the observed odd–even mass differences in the mass region. This choice of  $G_M$  is appropriate for the single-particle space employed in the PSM, where three major shells are used for each type of nucleons ( $N = 4, 5, 6$ , for neutrons and  $N = 3, 4, 5$ , for protons, a model space appropriate for normally deformed rare earth nuclei). The quadrupole pairing strength  $G_Q$  is assumed to be proportional to  $G_M$ , the proportionality constant being fixed as usual to be in the range 0.16–0.18. These interaction strengths are consistent with those used previously for the same mass region [10–12].

The Hamiltonian in Eq. (4) is diagonalized using the projected basis of Eq. (1). The obtained wave-function can be written as

$$\Psi_{IM}^\sigma = \sum_K f_{IK}^\sigma \hat{P}_{MK}^I |\Phi\rangle. \quad (6)$$

Note that, although only the qp-vacuum state is included in the basis in Eq. (1), its triaxial nature generates the  $K$ -state mixing when the diagonalization is carried out. The expansion coefficients  $f$ , obtained through the diagonalization of the shell-model Hamiltonian, describe the amount of  $K$ -mixing and specify various physical states (e.g., g-,  $\gamma$ -,  $\gamma\gamma$ -bands) [12]. The wave-function is then used to evaluate the electromagnetic transition probabilities. The reduced electric transition probabilities  $B(\text{EL})$  from an initial state  $(\sigma_i, I_i)$  to a final state  $(\sigma_f, I_f)$  are given by

$$B(\text{EL}, I_i \rightarrow I_f) = \frac{1}{2I_i + 1} |\langle \Psi_{I_f}^{\sigma_f} | \hat{Q}_L | \Psi_{I_i}^{\sigma_i} \rangle|^2, \quad (7)$$

and the reduced matrix element can be expressed as

$$\begin{aligned} & \langle \Psi_{I_f}^{\sigma_f} | \hat{Q}_L | \Psi_{I_i}^{\sigma_i} \rangle \\ &= \sum_{K_i, K_f} f_{I_i K_i}^{\sigma_i} f_{I_f K_f}^{\sigma_f} \sum_{M_i, M_f, M} (-)^{I_f - M_f} \\ & \quad \times \begin{pmatrix} I_f & L & I_i \\ -M_f & M & M_i \end{pmatrix} \\ & \quad \times \langle \Phi | \hat{P}_{K_f M_f}^{I_f} \hat{Q}_{LM} \hat{P}_{K_i M_i}^{I_i} | \Phi \rangle \\ &= 2 \sum_{K_i, K_f} f_{I_i K_i}^{\sigma_i} f_{I_f K_f}^{\sigma_f} \sum_{M', M''} (-)^{I_f - K_f} (2I_f + 1)^{-1} \end{aligned}$$

$$\begin{aligned} & \times \begin{pmatrix} I_f & L & I_i \\ -K_f & M' & M'' \end{pmatrix} \\ & \times \int d\Omega D_{M'' K_i}(\Omega) \langle \Phi | \hat{Q}_{LM'} \hat{R}(\Omega) | \Phi \rangle. \end{aligned}$$

The transition quadrupole moment  $Q_t(I)$  is related to  $B(\text{E}2)$  transition probability through

$$Q_t(I) = \sqrt{\frac{16\pi}{5}} \frac{\sqrt{B(\text{E}2, I \rightarrow I-2)}}{\langle I, 0, 2, 0 | I-2, 0 \rangle}. \quad (8)$$

In the calculation, we have used the standard effective charges of  $1.5e$  for protons and  $0.5e$  for neutrons [5,10].

The variation of  $Q_t$  as a function of spin  $I$  provides the information about the shape evolution of a rotating nucleus. In the simplest approximation for a nucleus as an axially deformed rigid body,  $Q_t$  has a constant value for all the spin states in a given band. In fact, for well deformed nuclei, one finds more or less a constant value of  $Q_t$  at low-spin states up to the first band-crossing region. Experimentally, deviations are observed from the rigid-body behavior in many nuclei at high-spin states, especially in the band-crossing region — one often observes a drop in  $Q_t$  due to small overlap between the wave-functions of the initial and the final states involved. It was shown [4] that the drop in  $Q_t$  in the band-crossing region cannot be quantitatively described by various types of cranking models where angular momentum is not treated as a good quantum number, but the calculations based on the projected shell model with axially symmetric basis can reproduce this phenomenon [5,6]. Very recently, it has been reported that angular momentum projection on the cranked HFB states can also describe the drop [7]. In the present work, we shall discuss the spin states below the band-crossing region.

The constant behavior of  $Q_t$  till the band-crossing region is noticed for most of the nuclei that are well deformed in the ground-state. In comparison, for some light rare-earth nuclei that belong to the transitional region, for instance,  $^{154-158}\text{Dy}$  and  $^{156-160}\text{Er}$ ,  $Q_t$  depicts a variation with angular momentum for the low-spin states of the g-band, well below the band crossing region. The existing experimental data seem to indicate a general trend of increasing  $Q_t$  for the spin region  $0 \leq I \leq 10$ . This variation of  $Q_t$  cannot

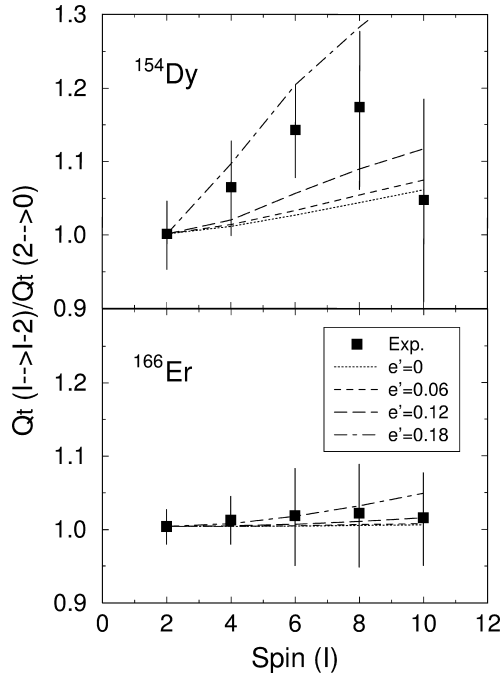


Fig. 1. Calculated transition quadrupole moments for the transitional nucleus  $^{154}\text{Dy}$  (top panel), and well-deformed nucleus  $^{166}\text{Er}$  (bottom panel) with different triaxial deformation  $\epsilon'$ . The corresponding experimental data [15,16] are also shown for a comparison.

be explained by calculations using the projected shell model with axially-symmetric basis [5,6].

In Fig. 1, the results of  $Q_t$  are presented for various values of the triaxial deformation parameter  $\epsilon'$  to investigate the dependence of  $Q_t$  on the triaxiality of the deformed Nilsson basis.  $\epsilon' = 0$  in Fig. 1 corresponds to the axially symmetric case. The calculated  $Q_t(I \rightarrow I-2)$  are normalized to the lowest transition  $Q_t(2 \rightarrow 0)$  in order to demonstrate more clearly any changes in  $Q_t$  as a function of spin.  $^{154}\text{Dy}$  has neutron number 88 and represents a transitional nucleus. Experimentally, a steady increase of  $Q_t$  has been observed for the several low-spin states [15] (the drop of  $Q_t$  at  $I = 10$  is due to the first band-crossing). As can be seen in the top panel of Fig. 1, this feature cannot be obtained when an axially symmetric basis ( $\epsilon' = 0$ ) is employed in the calculation. With increasing  $\epsilon'$  values, the calculated  $Q_t$  curves become steeper, and eventually the observed  $Q_t$  can be reproduced with  $\epsilon' \approx 0.15$ .

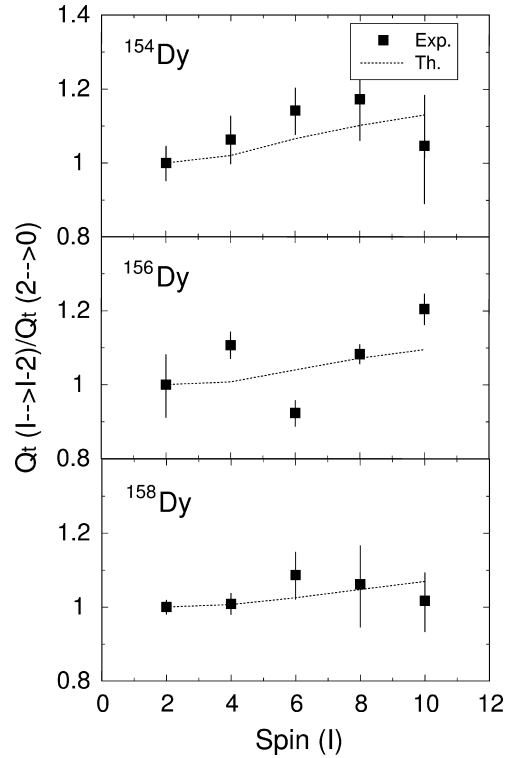


Fig. 2. Comparison of calculated transition quadrupole moments for  $^{154}, ^{156}, ^{158}\text{Dy}$  (dotted curves) with the available experimental data [15,17] (filled squares).

In the bottom panel of Fig. 1, similar calculations have been done for a well deformed nucleus  $^{166}\text{Er}$  having neutron number 98. The measured  $Q_t$  shows a rather constant behavior for the low-spin region [16]. It is interesting to observe very different calculated curves from those in the top panel of Fig. 1: with increasing  $\epsilon'$  values, the calculated  $Q_t$  curves keep showing a nearly constant behavior. Slightly enhanced values are obtained only with the largest  $\epsilon'$  in the calculation. We can thus conclude that the triaxial basis has no significant effect on the g-band properties for a well deformed nucleus that exhibits an axial rotor behavior near the ground-state.

In Figs. 2 and 3, the results of the TPMSM calculations are compared with the available experimental data for Dy- and Er-isotopes. In order to demonstrate the feature of increasing  $Q_t$ , we present them in the normalized form  $Q_t(I \rightarrow I-2)/Q_t(2 \rightarrow 0)$  as in Fig. 1. (We would like to add that our calculations also

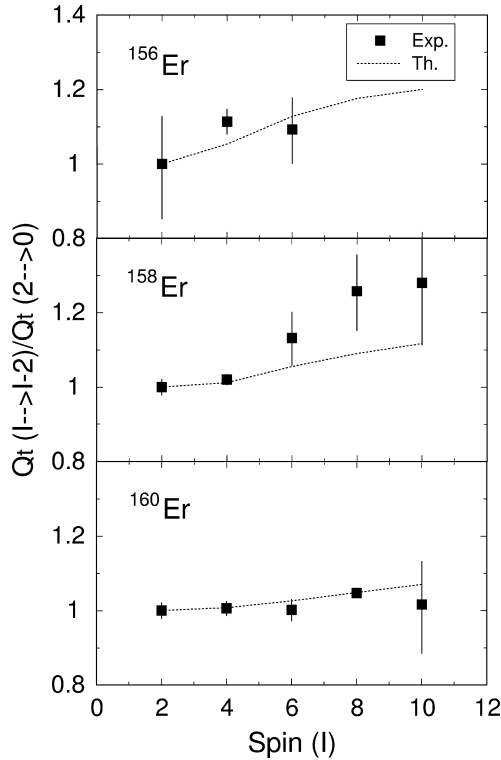


Fig. 3. Comparison of calculated transition quadrupole moments for  $^{156,158,160}\text{Er}$  (dotted curves) with the available experimental data [18–20] (filled squares).

reproduce the absolute values of  $Q_t$  for all the nuclei studied quite accurately.) It is found that by employing a triaxial deformation  $\epsilon' \approx 0.15$ , the observed feature of the  $Q_t$ 's can be reproduced reasonably well in most of the cases. At this stage, a fine adjustment of  $\epsilon'$  in the calculations for each individual nucleus is not necessary since in many of the data discussed here, the experimental uncertainties are quite large.

As is clear in Fig. 2, the experimental  $Q_t$  for  $^{154}\text{Dy}$  [15] can be nicely reproduced till  $I = 8$ . This was not possible in the projected shell model calculations if axially deformed basis was used [5,6]. The general feature of the observed  $Q_t$  for  $^{156}\text{Dy}$  [17] also shows an increasing trend with increasing spin, which is described by the present calculations. The physical reasons for a sudden drop in the experimental  $Q_t$  at  $I = 6$  are unclear. In  $^{158}\text{Dy}$ , the increase in the experimental  $Q_t$  [17] is not as significant as in the two lighter isotopes. This feature has also been reproduced

in our calculations with the same  $\epsilon'$  used for the  $^{154}\text{Dy}$  and  $^{156}\text{Dy}$  calculations.

The results for three light Er-isotopes are presented in Fig. 3. The experimental  $Q_t$  of the first three spin-states in  $^{156}\text{Er}$  [18] exhibit an increasing trend in  $Q_t$  as a function of spin, which is correctly described by the calculation. The  $Q_t$  for  $^{158}\text{Er}$  were measured in Ref. [19] up to very high-spin states. The data clearly depict an increasing trend, which is reasonably described by the calculation. The data for  $^{160}\text{Er}$  [20] depict nearly constant values for the three low-spin states, with slight variations for  $I = 8$  and 10. The agreement of our calculation for this nucleus is also satisfactory. We remark that with the configuration space and interaction strengths employed in the present work, the calculated moments of inertia for the g-bands and the calculated spectra for the multi-phonon  $\gamma$ -vibrational bands were shown to agree well with the observed data [11,12].

The behavior of  $Q_t$  as a function of angular momentum may provide a measure of the triaxiality for a nuclear system. For the transitional nuclei studied in the present work, larger increase in  $Q_t$  with angular momentum corresponds to higher values of triaxiality used in the basis. The triaxial deformation parameter  $\epsilon'$  is approximately related to the conventional triaxial parameter  $\gamma$  through the relation  $\tan \gamma = \frac{\epsilon'}{\epsilon}$ . The value of  $\epsilon$  is held fixed for each nucleus in the calculations, and therefore,  $\gamma$  increases linearly with  $\epsilon'$ . For those well deformed nuclei, the dependence of  $Q_t$  on the basis triaxiality is insensitive. Therefore, the g-band  $Q_t$  alone are not sufficient to determine triaxiality for a well deformed nucleus, and additional physical quantities must be supplied [16,21].

In conclusion, the low-spin transition quadrupole moments of the ground-state bands in  $\gamma$ -soft nuclei have been studied using the triaxial projected shell model approach. The shell model diagonalization is carried out with three-dimensional angular momentum projection based on the triaxial deformed Nilsson-states. It has been shown that for transitional nuclei, the rotational evolution of the transition quadrupole moments depends sensitively on triaxial deformation of the mean-field potential.

The development of the three-dimensional angular momentum projection method for the electromagnetic transition calculations has opened possibility of the application of the projected shell model approach

to a wide range of problems. The next important application would be the study of the inter-band transitions between the ground-state band and the  $\gamma$ -bands. This work is presently being pursued and the results will be published in the near future.

## References

- [1] A. Bohr, B.R. Mottelson, *Nuclear Structure*, Vol. II, Benjamin, New York, 1975.
- [2] H. Schatz et al., *Phys. Rep.* 294 (1998) 167.
- [3] F. Xu, P.M. Walker, J.A. Sheikh, R. Wyss, *Phys. Lett. B* 435 (1998) 257.
- [4] M.L. Cescato, Y. Sun, P. Ring, *Nucl. Phys. A* 533 (1991) 455.
- [5] Y. Sun, J.L. Egido, *Nucl. Phys. A* 580 (1994) 1.
- [6] V. Velázquez, J. Hirsch, Y. Sun, M. Guidry, *Nucl. Phys. A* 653 (1999) 355.
- [7] K. Enami, K. Tanabe, N. Yoshinaga, *Phys. Rev. C* 61 (1999) 027301.
- [8] K. Kumar, M. Baranger, *Nucl. Phys. A* 110 (1968) 529.
- [9] K. Hara, A. Hayashi, P. Ring, *Nucl. Phys. A* 385 (1982) 14.
- [10] K. Hara, Y. Sun, *Int. J. Mod. Phys. E* 4 (1995) 637.
- [11] J.A. Sheikh, K. Hara, *Phys. Rev. Lett.* 82 (1999) 3968.
- [12] Y. Sun, K. Hara, J.A. Sheikh, J. Hirsch, V. Velázquez, M. Guidry, *Phys. Rev. C* 61 (2000) 064323.
- [13] S.G. Nilsson et al., *Nucl. Phys. A* 131 (1969) 1.
- [14] R. Bengtsson, S. Frauendorf, F.-R. May, *At. Data Nucl. Data Tables* 35 (1986) 15.
- [15] F. Azgui et al., *Nucl. Phys. A* 439 (1985) 573.
- [16] C. Fahlander et al., *Nucl. Phys. A* 537 (1992) 183.
- [17] H. Emling et al., *Nucl. Phys. A* 419 (1984) 187.
- [18] R.G. Helmer, *Nucl. Data Sheets* 65 (1992) 65.
- [19] M. Oshima et al., *Phys. Rev. C* 33 (1986) 1988.
- [20] C.W. Reich, *Nucl. Data Sheets* 78 (1996) 547.
- [21] P. Ring, A. Hayashi, K. Hara, H. Emling, E. Grosse, *Phys. Lett. B* 110 (1982) 423.